Electronic Supplementary Material (ESI) for Journal of Materials Chemistry A.

Supporting Information

Interfacial Nickel Nitride/Sulfide as a Bifunctional Electrode for Highly Efficient Overall Water/Seawater Electrolysis

Yongqiang Zhao[a], Bo Jin[a], Anthony Vasileff[a], Yan Jiao[a], Shi-Zhang Qiao*[ab]

[a.] School of Chemical Engineering, The University of Adelaide, Adelaide, SA 5005, Australia, E-mail: s.qiao@adelaide.edu.au

[b.] School of Materials Science and Engineering, Tianjin University, Tianjin, 300072, China

Experimental

Chemicals: Nickel foam (thickness 1.6 mm, 95%), thiourea (≥99.0%), sulphur (≥99.0%), phosphate buffer solution (1.0 M, pH=7.4) and nickel hydroxide (99%) were purchased from Sigma-Aldrich and used without further purification, except for the nickel foam. Milli-Q water (18.2 M Ωcm, PURELAB Option-Q) was used in all experiments. The nickel foam was washed with dilute HCl, ultrapure water, acetone and ethanol, and dried in vacuum at 25 °C before use.

Fabrication of the interfacial nickel nitride and sulfide electrode (NiNS): The NiNS electrode was fabricated by a one-step calcination of nickel foam with thiourea in a vacuum sealed ampoule. In a typical synthesis, a pre-cleaned piece of Ni foam (20.60 mg, 1.5 cm × 0.3 cm × 0.16 cm, length × width × height) and thiourea (6.14 mg) were sealed in an ampoule under vacuum and then calcinated at 550 °C for 5 h. The heating rate was 5 °C min^{-1} and the cooling process took place naturally. The mass ratio of Ni foam and thiourea was 1:0.298. The loading of nickel nitride and sufide was calculated to be 9.27 and 10.68 mg, respectively. The NiNS electrode was washed with ethanol and dried in vacuum at 25 °C before use.

Fabrication of Pt-C and Ir-C Loaded Electrodes: 4 mg Pt-C or Ir-C were dispersed in 1 mL water, followed by sonication for 30 min to obtain a homogeneous catalyst ink. 150 μL of the catalyst ink and 40 μL 2% Nafion solution were loaded in succession on the surface of Ni foam (surface area: 0.6 cm^2). The overall loading amount was 1 mg cm^{-2}.

Fabrication of nickel nitride: Nickel nitride (Ni_3N) was fabricated according to a modified method from previous literature.[S1] In a typical synthesis, 10 mg of nickel hydroxide was place in a tube furnace and heated to 390 °C under NH_3 flow (1 bar, 400 sccm) to prepare black Ni_3N.

Fabrication of nickel sulfide: Nickel sulfide (Ni_3S_2) was fabricated by a one-step calcination of nickel foam with sulfur in a vacuum sealed ampoule. In a typical synthesis, a pre-cleaned piece of Ni foam (20.60 mg, 1.5 cm × 0.3 cm × 0.16 cm, length × width × height) and sulfur (2.58 mg) were sealed in an ampoule under vacuum and then calcinated at 500 °C for 5 h. The heating rate was 5 °C min^{-1} and the cooling process took place naturally. The nickel sulfide was washed with ethanol and dried in vacuum at 25 °C before use.

Fabrication of mechanically mixed Ni_3N and Ni_3S_2 electrode (MNiNS): 103 mg Ni_3N and 118.67 mg Ni_3S_2 were were dispersed in 1 mL 2% Nafion aqueous solution, followed by sonication for 30 min to obtain a homogeneous catalyst ink. 200 μL of the catalyst ink was loaded on the surface of pre-cleaned Ni foam (surface area: 1 cm^2). The as-prepared MNiNS electrode was dried at 40 °C in vacuum. The overall loading amount was 9.27 mg of Ni_3N and 10.68 mg of Ni_3S_2, respectively.

Electrochemical Characterization: HER and OER measurements were performed on a CHI 760 D Bipotentiostat (CH Instruments, Inc., USA) in Ar or O_2 saturated 1.0 M KOH aqueous solution using a conventional three-electrode system with a graphite rod as the counter electrode and Ag/AgCl (4 M KCl) as the reference electrode. Overall water splitting measurements were performed in a three-electrode glass cell. The phosphate buffer solution was used for overall water electrolysis in neutral pH conditions. To investigate the performance of the systems in seawater, neutral-buffered seawater electrolyte was prepared. Natural seawater was collected from Glenelg beach in Adelaide, Australia, and was applied directly without further purification. The neutral-buffered seawater electrolyte was prepared by mixing phosphate buffer solution with natural seawater, and the pH of the mixed electrolyte was adjusted to 7.05. The current density was normalized to the geometric surface area and the measured potentials versus Ag/AgCl were converted to the reversible hydrogen electrode (RHE) scale according to the Nernst equation:

$$E_{RHE} = E_{Ag/AgCl} + 0.059 \times pH + 0.205 \quad (1)$$

The polarization curves were recorded in the range of 1.0-1.8 V vs. RHE for the OER and -0.6 to 0 V vs. RHE for the HER at a slow scan rate of 5 mV s^{-1} to minimize the capacitive current. The working electrodes were scanned for several times until the signals were stabilized, and then the data for polarization curves were collected and corrected for the iR contribution within the cell. The stability test was conducted using a controlled-potential electrolysis method without iR compensation. The EIS was obtained by AC impedance spectroscopy within the frequency range from 0.01 to 100 kHz in 1.0 M KOH. The equivalent circuit for fitting of the EIS data was achieved with ZView software. The Tafel slope was calculated according to Tafel equation as follows:

$$\eta = b\log(j/j_0) \quad (2)$$

where η denotes the overpotential, b denotes the Tafel slope, j denotes the current density, and j_0 denotes the exchange current density. The onset potentials were determined based on the beginning of the linear region in the Tafel plots. The overpotential was calculated as follows:

$$\eta = E \text{ (vs RHE)} - Er \text{ (vs RHE)} \quad (3)$$

where E denotes the actual applied potential and Er denotes the reversible potential of the reaction. *E*r is 1.23 V versus RHE for the OER and 0 V vs. RHE for the HER. HER η is always negative. The electrochemical surface area of the electrodes was related to double layer charging curves using cyclic voltammetry in the potential range 0.72 - 0.82 V vs. RHE. The double-layer capacitance values were determined from the slope of the capacitive current versus the scan rate.

Physicochemical Characterization: STEM images and corresponding mapping images were obtained on an FEI Titan Themis 80-200 system. Transmission electron microscopy (TEM) images and the selected area electron diffraction (SAED) patterns were obtained on a JEOL 2100F microscope at an acceleration voltage of 200 kV. High resolution TEM (HRTEM) images were obtained on a Philips CM200 microscope at an acceleration voltage of 200 kV. Scanning electron microscopy (SEM) images were collected on the FEI Quanta 450 at high vacuum with an accelerating voltage of 30 kV. X-ray diffraction (XRD) patterns were collected on a powder X-ray diffractometer at 40 kV and 15 mA using Co-Kα radiation (Miniflex, Rigaku). X-ray photoelectron spectra (XPS) were obtained using an Axis Ultra (Kratos Analytical, UK) XPS spectrometer equipped with an Al Kα source (1486.6 eV). The composition of NiNS was determined by element analysis (vario EL cube, ELE-MENTAR).

Supplementary Results

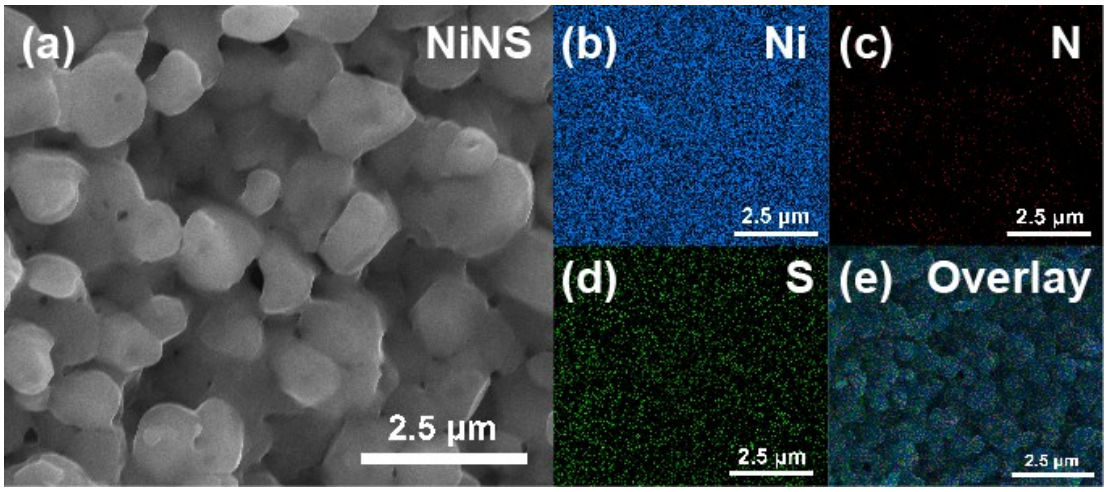

Fig. S1 (a) SEM image of NiNS. Corresponding mapping of (b) Ni, (c) N, (d) S, and (e) overlay.

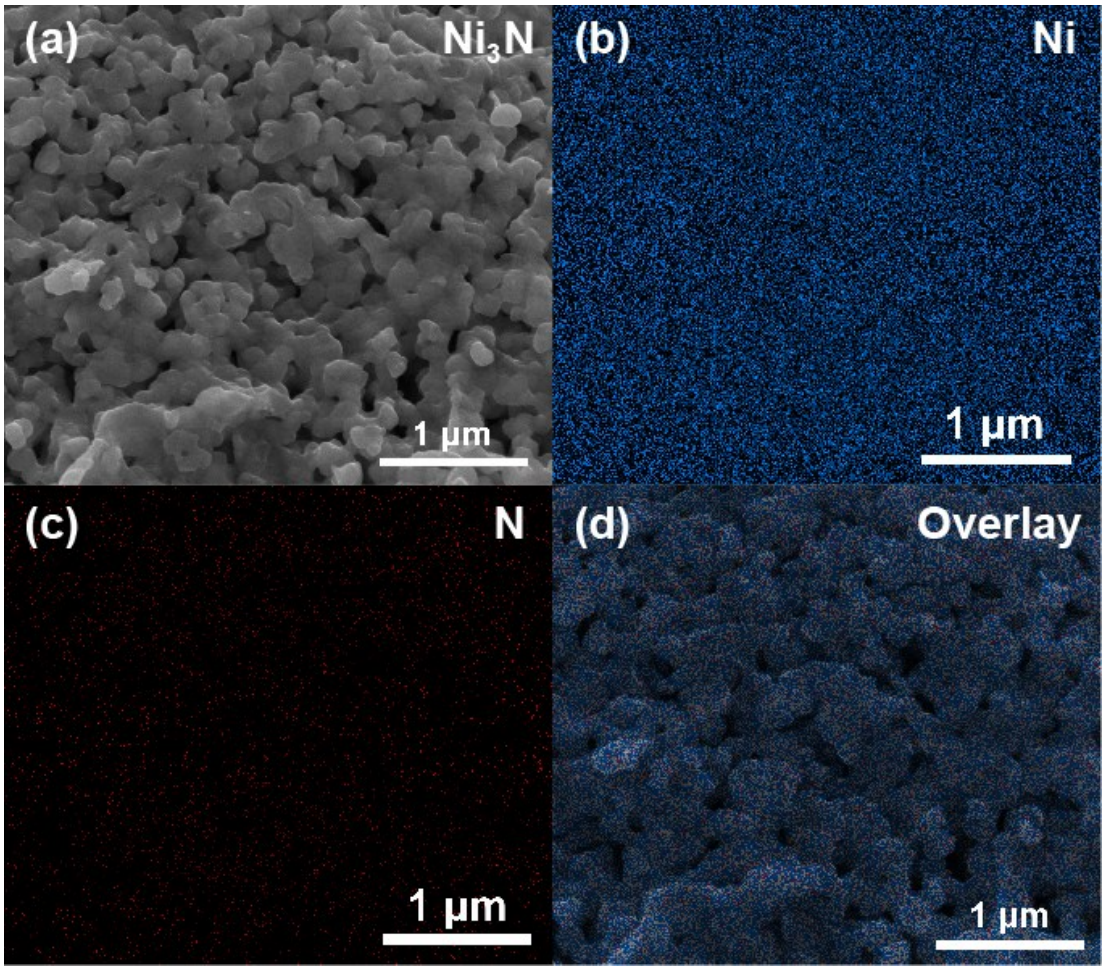

Fig. S2 (a) SEM image of nickel nitride. Corresponding mapping of (b) Ni, (c) N, and (d) overlay.

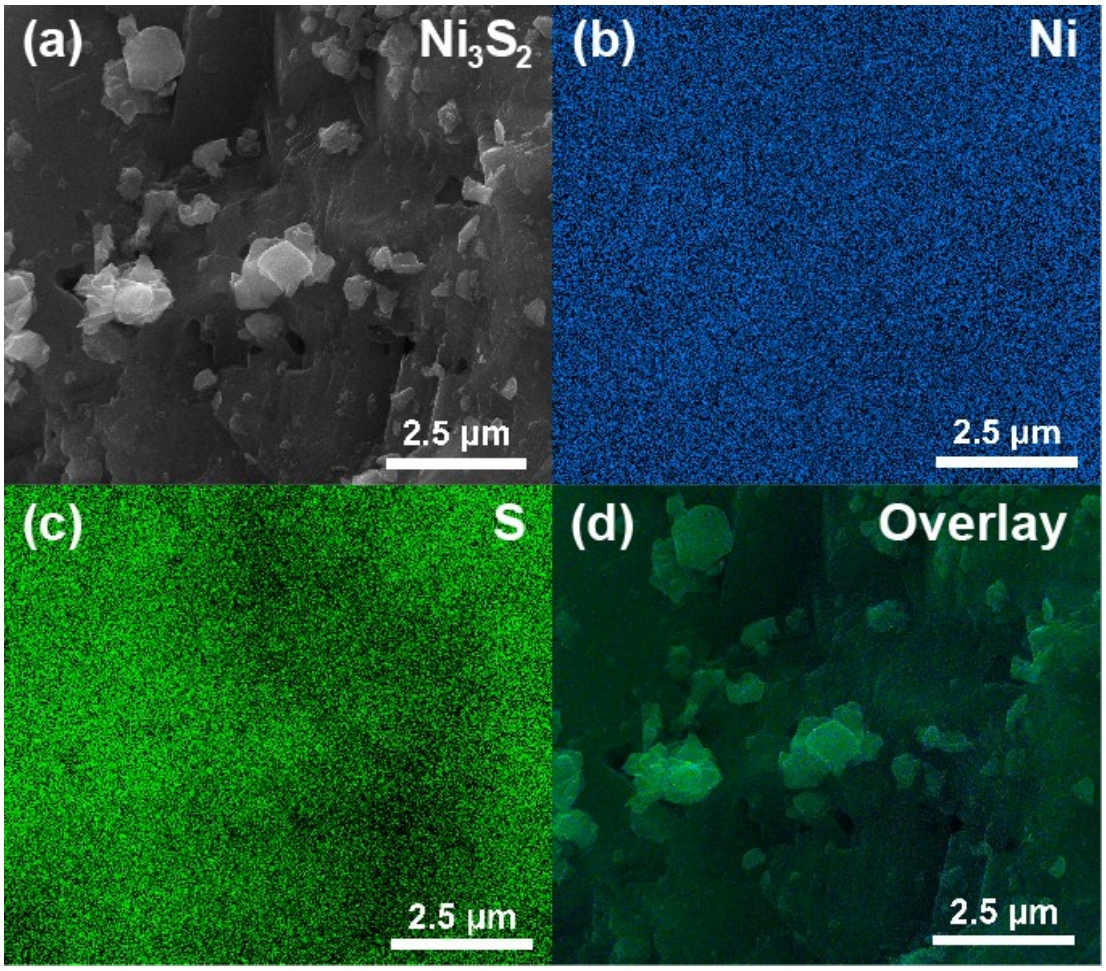

Fig. S3 (a) SEM image of nickel sulfide. Corresponding mapping of (b) Ni, (c) S, and (d) overlay.

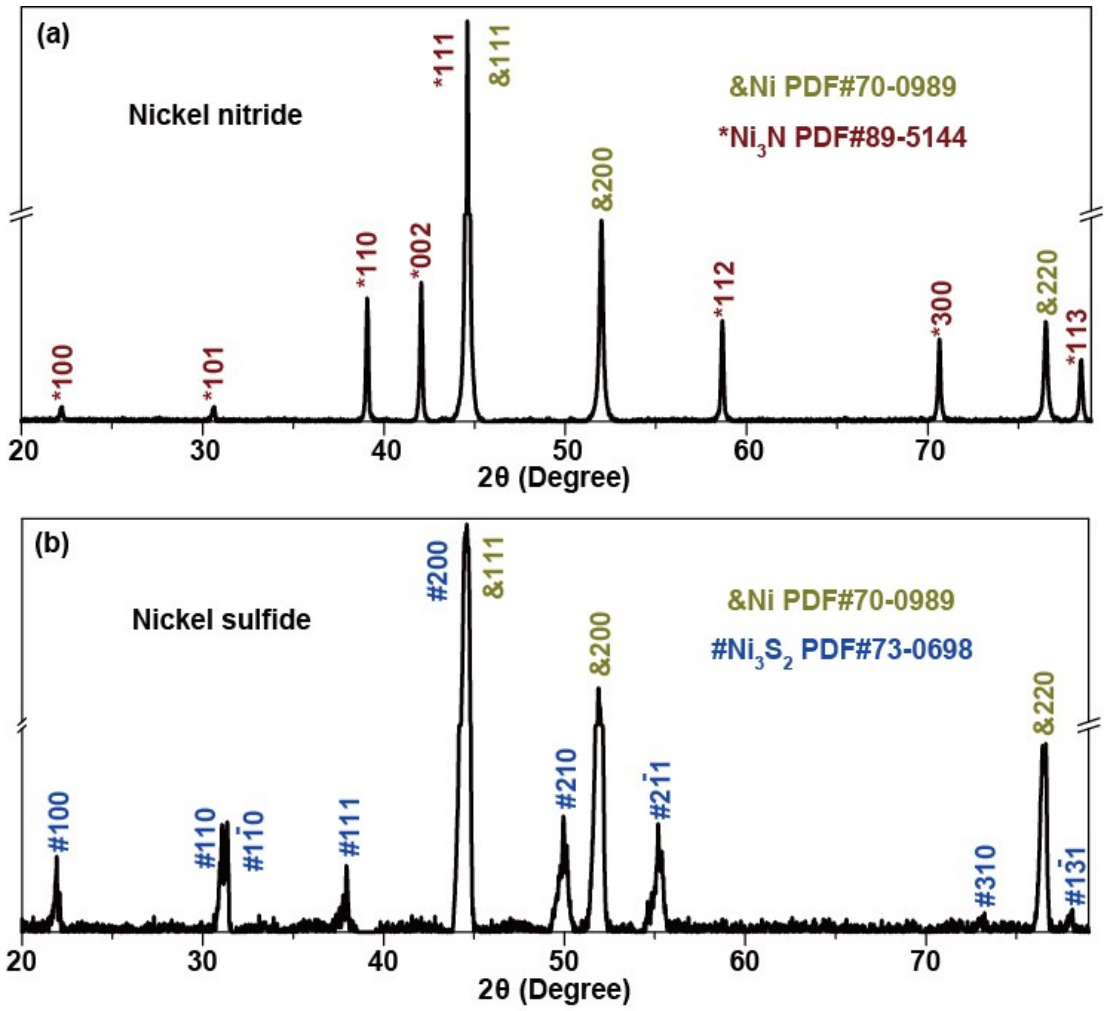

Fig. S4 XRD patterns of (a) nickel nitride and (b) nickel sulfide.

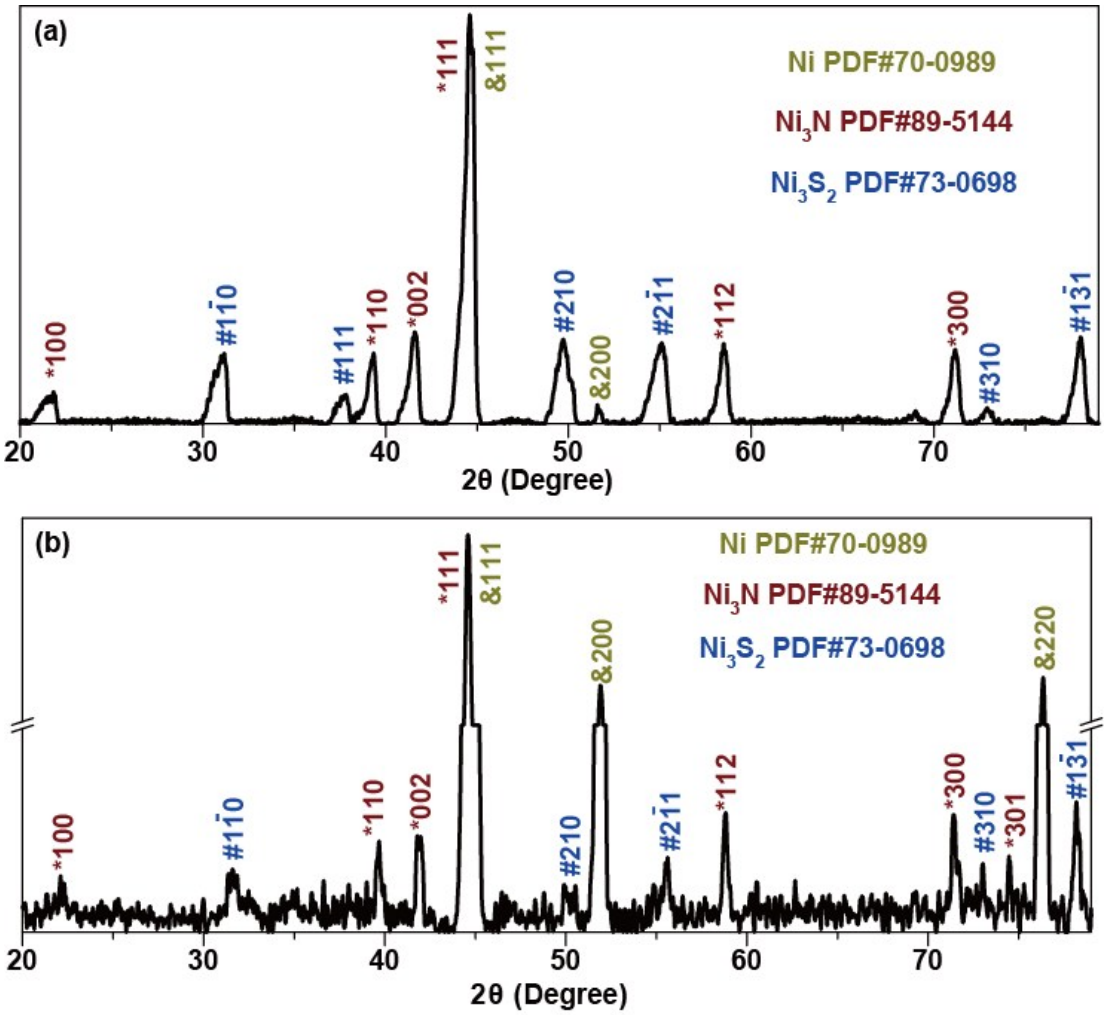

Fig. S5 XRD patterns of NiNS after 12 h continuous (a) HER and (b) OER operation.

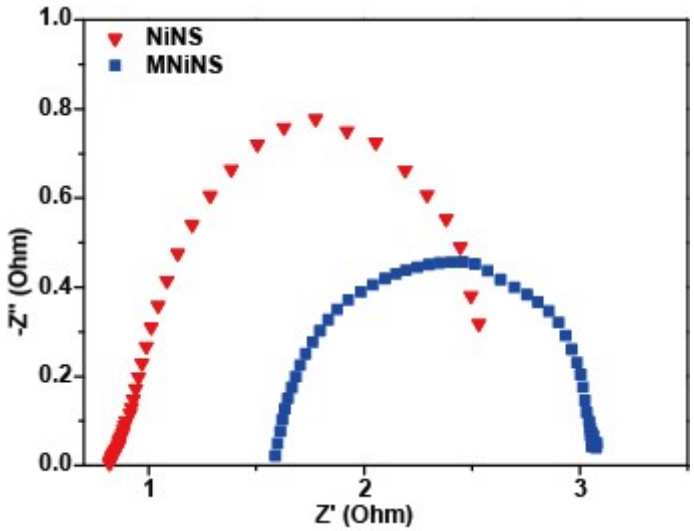

Fig. S6 Nyquist plots of NiNS and MNiNS electrodes in 1.0 M KOH with the potential of -1.31 V vs. RHE.

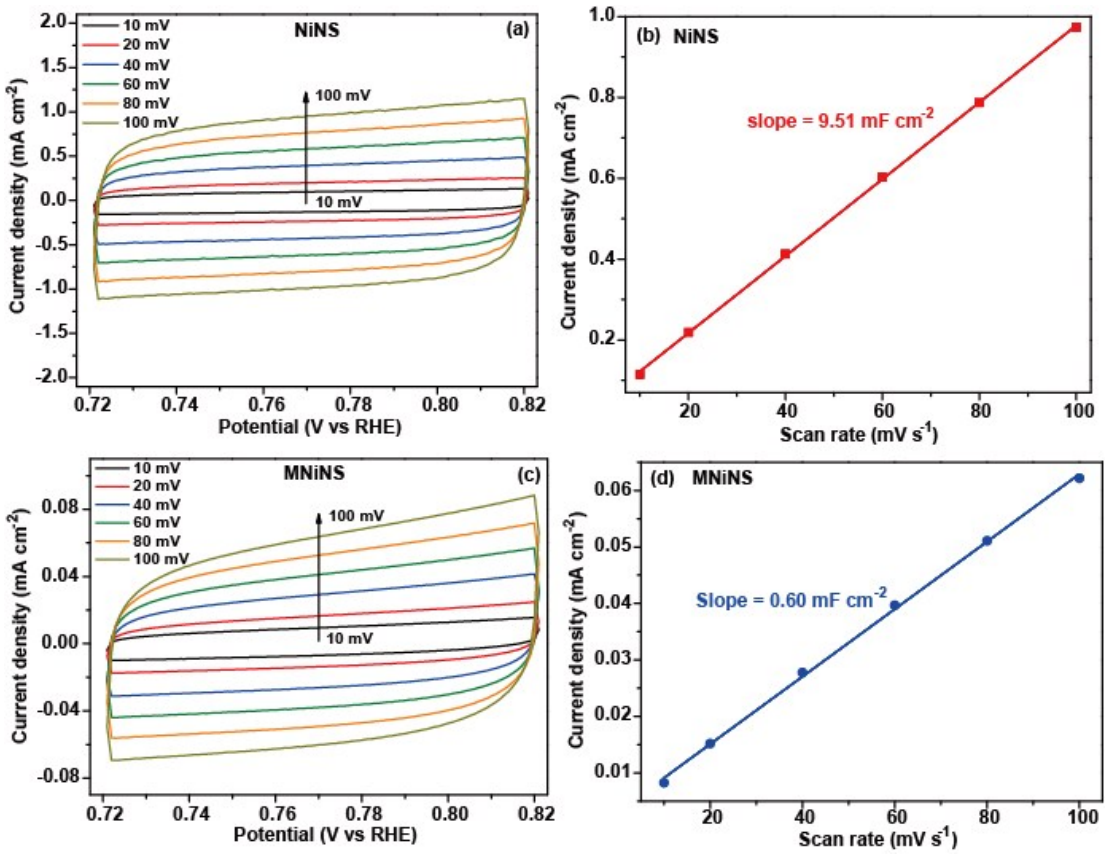

Fig. S7 The double-layer region with scan rates ranging from 10 to 100 mV s^{-1} in 1.0 M KOH for (a) NiNS and (c) MNiNS. Charging current density with different scan rates for (b) NiNS and (d) MNiNS.

Table S1 Element analysis of NiNS, Ni_3N and Ni_3S_2

	Nickel (wt.%)[1]	Nitrogen (wt.%)	Sulfur (wt.%)
NiNS	87.18	4.17	8.65

[1]By difference

Table S2 HER performance comparison between NiNS and recently reported electrocatalysts in alkaline media

Electrocatalysts	Electrolyte	j, mA cm^{-2}	η required, mV	Tafel slop, mV dec^{-1}	Reference
NiNS	1.0 M KOH	100	197		This work
Ni_3N-Co	1.0 M KOH	100	290	156	S2
NiMoN/Ni_3N on carbon cloth	1.0 M KOH	100	200	64	S3
Ni_2P@NPCNFs	1.0 M KOH	100	205	79.7	S4
$Ni_xCo_{3-x}S_4/Ni_3S_2$/NF	1.0 M KOH	100	258	107	S5
Co_3Se_4 nanowires on Co foam	1.0 M KOH	100	262	72	S6
200-SMN/NF	1.0 M KOH	100	287	72.9	S7
$Pr_{0.5}(Ba_{0.5}Sr_{0.5})_{0.5}Co_{0.8}Fe_{0.2}O_{3-\delta}$	1.0 M KOH	100	310	45	S8
$NiCo_2O_4$ nanowire arrays on nickel foam	1.0 M KOH	100	275	88	S9
$NiCo_2O_4$ hollow microcuboids	1.0 M NaOH	100	245	49.7	S10
Ni_3N nanosheets on carbon cloth	1.0 M KOH	100	470	N/A	S11

Table S3 OER performance comparison between NiNS and recently reported electrocatalysts in alkaline media

Electrocatalysts	Electrolyte	j, mA cm^{-2}	η required, mV	Tafel slop, mV dec^{-1}	Reference
NiNS	1.0 M KOH	100	404		This work
MoS_2/NiS NCs	1.0 M KOH	100	~475	53	S12
NCP/G NSs	1.0 M KOH	100	400	65.9	S13
NF@Ni/C-600	1.0 M KOH	100	~460	54	S14
Ni_3S_2/NF-2	1.0 M KOH	100	425	N/A	S15
Fe_1-$(Co_3O_4)_{10}$ holy nanosheets	1.0 M KOH	100	~410	55	S16
$NiCo_2O_4$@$CoMoO_4$/NF-7	1.0 M KOH	100	~510	102	S17
Ni-Mo_xC/NC-100	1.0 M KOH	100	470	74	S18
NiSe-$Ni_{0.85}Se$/CP	1.0 M KOH	100	420	75	S19
NiMoN-NF700	1.0 M KOH	100	~405	54	S20
$NiCo_2O_4$ nanowire arrays	1.0 M KOH	100	470	66.9	S9

Reference

[S1] K. Xu, P. Chen, X. Li, Y. Tong, H. Ding, X. Wu, W. Chu, Z. Peng, C. Wu,Y. Xie, *J. Am. Chem. Soc.* **2015,** *137*, 4119.

[S2] C. Zhu, A.-L. Wang, W. Xiao, D. Chao, X. Zhang, N. H. Tiep, S. Chen, J. Kang, X. Wang, J. Ding, J. Wang, H. Zhang, H. J. Fan, *Adv. Mater.* **2018,** *30*, 1705516.

[S3] A. Wu, Y. Xie, H. Ma, C. Tian, Y. Gu, H. Yan, X. Zhang, G. Yang, H. Fu, *Nano Energy* **2018,** *44*, 353.

[S4] M.-Q. Wang, C. Ye, H. Liu, M. Xu, S.-J. Bao, *Angew. Chem., Int. Ed.* **2018,** *57*, 1963.

[S5] Y. Wu, Y. Liu, G.-D. Li, X. Zou, X. Lian, D. Wang, L. Sun, T. Asefa, X. Zou, *Nano Energy* **2017,** *35*, 161.

[S6] W. Li, X. Gao, D. Xiong, F. Wei, W.-G. Song, J. Xu, L. Liu, *Adv. Energy Mater.* **2017**, 7, 1602579.

[S7] Z. Cui, Y. Ge, H. Chu, R. Baines, P. Dong, J. Tang, Y. Yang, P. M. Ajayan, M. Ye, J. Shen, *J. Mater. Chem. A* **2017,** *5*, 1595.

[S8] X. Xu, Y. Chen, W. Zhou, Z. Zhu, C. Su, M. Liu, Z. Shao, *Adv. Mater.* **2016,** *28*, 6442.

[S9] A. Sivanantham, P. Ganesan,S. Shanmugam, *Adv. Funct. Mater.* **2016,** *26*, 4661.

[S10] X. Gao, H. Zhang, Q. Li, X. Yu, Z. Hong, X. Zhang, C. Liang, Z. Lin, *Angew. Chem., Int. Ed.* **2016,** *55*, 6290.

[S11] D. Gao, J. Zhang, T. Wang, W. Xiao, K. Tao, D. Xue, J. Ding, *J. Mater. Chem. A* **2016,** *4*, 17363.

[S12] Z. Zhai, C. Li, L. Zhang, H.-C. Wu, L. Zhang, N. Tang, W. Wang, J. Gong, *J. Mater. Chem. A* **2018,** *6*, 9833.

[S13] J. Tian, J. Chen, J. Liu, Q. Tian, P. Chen, *Nano Energy* **2018,** *48*, 284.

[S14] H. Sun, Y. Lian, C. Yang, L. Xiong, P. Qi, Q. Mu, X. Zhao, J. Guo, Z. Deng, Y. Peng, *Energy. Environ. Sci.* **2018,** *11*, 2363.

[S15] G. Liu, Z. Sun, X. Zhang, H. Wang, G. Wang, X. Wu, H. Zhang, H. Zhao, *J. Mater. Chem. A* **2018,** *6*, 19201.

[S16] Y. Li, F.-M. Li, X.-Y. Meng, X.-R. Wu, S.-N. Li, Y. Chen, *Nano Energy* **2018,** *54*, 238.

[S17] Y. Gong, Z. Yang, Y. Lin, J. Wang, H. Pan, Z. Xu, *J. Mater. Chem. A* **2018,** *6*, 16950.

[S18] D. Das, S. Santra, K. K. Nanda, *ACS Appl. Mater. Interfaces* **2018,** *10*, 35025.

[S19] Y. Chen, Z. Ren, H. Fu, X. Zhang, G. Tian, H. Fu, *Small* **2018,** *14*, 1800763.

[S20] B. Chang, J. Yang, Y. Shao, L. Zhang, W. Fan, B. Huang, Y. Wu, X. Hao, *ChemSusChem* **2018,** *11*, 3198.